Published as: van der Westhuizen, I. and W.W. Focke, Stabilizing sunflower biodiesel with synthetic antioxidant blends. Fuel, 2018. 219: p. 126-131. https://doi.org/10.1016/j.fuel.2018.01.086

Stabilizing Sunflower biodiesel with synthetic antioxidant blends

Isbé van der Westhuizen[a], Walter W Focke[a,*]

[a]Institute of Applied Materials, Department of Chemical Engineering, University of Pretoria, Private bag X20, Hatfield 0028, South Africa

Highlights

- Sunflower biodiesel stabilized with three different types of synthetic antioxidant.
- Rancimat induction periods (IP) estimated from conductivity vs. time responses.
- IP from second derivative method exceeded that from common tangent method.
- Amine- and phenolic-based antioxidants combinations showed synergistic activity.
- Best stabilisation results were obtained with pyrogallol.

Abstract

Biodiesel was prepared using base catalyzed methanolysis of sunflower oil. The oxidative stability of the neat biodiesel, as well as samples spiked with 0.15 wt.% antioxidant was quantified by induction periods (*IP*) obtained with the Rancimat method according to the tangent method. The neat stabilizers, binary blends and a ternary mixture of poly(1,2-dihydro-2,2,4-trimethylquinoline) (Orox PK), tetrakis[methylene(3,5-di-t-butyl-4-hydroxyhydrocinnamate)]methane (Anox 20), and tris(nonylphenyl)phoshite (Naugard P) were tested. Of these, Anox 20 was the most effective stabilizer while Naugard P proved ineffective for the sunflower biodiesel. Synergistic improvement of oxidative stability was observed on partial substitution of this phenolic-based compound with the Orox PK. Combinations of the latter amine-based stabilizer with other phenolic antioxidants did not show any synergy, with perhaps the exception of DTBHQ. At a dosage of 0.15 wt.%, only TBHQ, propyl gallate and pyrogallol, as well as their 2:1 blends with Orox PK, provided *IP* values that exceeded 8 h as required by the European Standard EN 14214 for biodiesel.

Graphical abstract

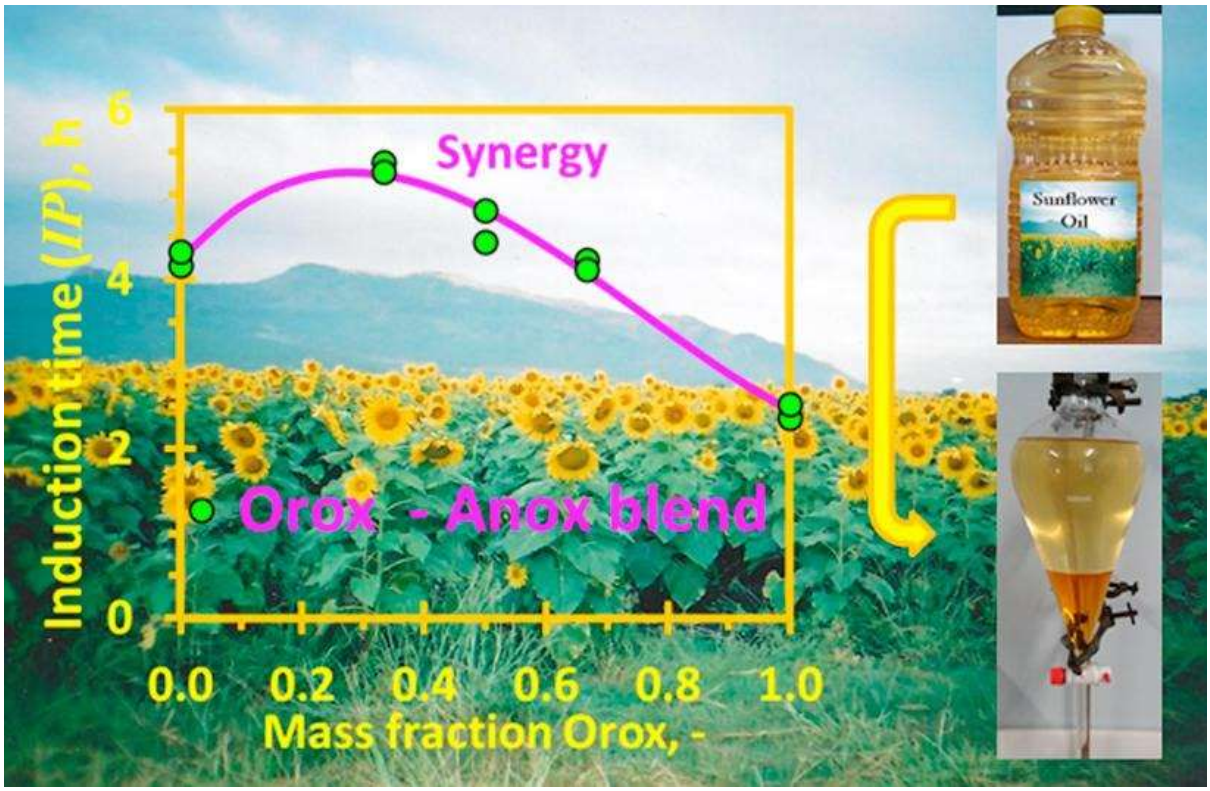

KEYWORDS: Antioxidant; biodiesel; oxidative stability; Rancimat method; Scheffé polynomial

1. Introduction

Biodiesel is a renewable fuel produced by the methanolysis of vegetable oil or animal fat in the presence of a catalyst (usually an alkali) to produce fatty acid methyl esters (FAME). The presence of unsaturation on the long-chain fatty acid makes it much more susceptible to oxidative degradation than synthetic petroleum diesel [1, 2]. Oxidation commences as soon as the biodiesel has been produced and continues during long term storage. The oxidative stability can be improved by adding suitable antioxidants [2-4]. The effectiveness of a synthetic antioxidant depends on its chemical structure as well as the compounds present in the biodiesel. Antioxidants act by interrupting the degradation process and they are usually consumed in the course of stabilization. Primary antioxidants terminate the propagation reaction by a chain

breaking mechanism. Primary antioxidants typically are hydrogen donors (e.g. phenolic hydroxyl groups) that trap the free radicals formed by the degradation reaction. They inhibit oxidation by donating the hydrogen from the hydroxyl group to the free radical present [5]. Amine-based primary oxidants are also known but most studies on vegetable oils and other ester derivatives are limited to the phenolic types. Secondary antioxidants are hydroperoxide decomposers and include organic sulfur or phosphorus compounds [2, 3, 6-8]. They function by converting the hydroperoxides to inactive non-radical compounds such as alcohols.

Some antioxidants combinations show synergistic activity [5, 9, 10]. According to Ingold [11] synergism can arise when the two component antioxidants perform different roles during inhibition. A few studies explored this avenue for improving the oxidative stability of FAME. Examples include *tert*-butyl hydroquinone (TBHQ) combinations with butylated hydroxyanisole (BHA), propyl gallate (PG) and pyrogallol (PY) and α-tocopherol with myricetin. In these instances the mechanism appears to involve the regeneration of the more efficient oxidant by the other one [12].

EN14112 [13] is currently the preferred procedure for determining the oxidative stability of biodiesel. This is quantified by the induction time measured with a Rancimat instrument. In this method, a constant flow of air is passed through a small biodiesel sample held at 110°C. During an initial induction phase virtually no secondary products are formed. This is abruptly followed by an oxidation phase characterized by a rapid increase in peroxide value and the formation of volatile products, mainly formic acid and acetic acid. These volatile acids are transported via the stream of air into a measuring cell filled with deionized water. The volatile acids formed during the oxidation process dissolve in the deionized water and increase its conductivity. This increase in conductivity is measured as a function of time in the Rancimat method. The induction time (*IP*) is then evaluated from the experimental conductivity *vs*. time curve.

Compared to other biodiesels, the one derived from sunflower oil is particularly prone to oxidative degradation [14]. Hence, the main objective of this study was to study the stabilization of sunflower oil-based biodiesel. Secondly, it was of interest to determine whether synergistic activity occurs in mixtures of phenolic-, phosphite- and amine-based antioxidants. Therefore, such combinations were explored using the Rancimat method while keeping the overall antioxidant concentration fixed at 0.15 wt.%. The aims were (a) to determine whether antioxidants commonly used in polyolefin polymers such as polyethylene (which features no double bonds) and in natural rubber where there are numerous double bonds present have any merit as biodiesel stabilisers, and (b) to establish whether synergistic effects are present when they are used in suitable combinations.

2. Experimental

2.1 Materials

Pure, triple-distilled sunflower oil was supplied by Sunfoil. Three different stabilizer chemistries were explored namely phenol-, amine- and phosphite-based antioxidants. A comprehensive study was done on combinations of tetrakis[methylene(3,5-di-t-butyl-4-hydroxyhydrocinnamate)]methane (Anox 20 ex Addivant) a hindered phenolic antioxidant, poly(1,2-dihydro-2,2,4-trimethylquinoline) (Orox PK ex Orchem) an amine-type antioxidant and tris(nonylphenyl) phosphite (Naugard P ex Chemtura) a phosphite-type antioxidant. The latter is classed as a secondary antioxidant while the first two are considered to be primary antioxidants. The antioxidants were added to the biodiesel at a total loading of 0.15 wt.%. Both binary as well as a ternary blends of these antioxidants were evaluated. Additional combinations of the amine with other phenol-type antioxidants were tested at the 1:2 mass ratio. SigmaAldrich supplied samples of BHT, pyrogallol and propyl gallate while TBHQ and

DTBHQ were obtained from Aromas and Fine Chemicals, South Africa. All chemicals were used as received, i.e. without further purification.

2.2 Biodiesel preparation

The biodiesel was prepared using alkali catalyzed methanolysis as described previously [15]. Potassium hydroxide was used as the catalyst and several small batches of 500 mL each were prepared and subsequently combined before testing and analysis.

2.3 Characterization

The FAME analysis for sample BD01 was performed by the CSIR Food and Beverage Laboratory (now acquired by Aspirata Certification Auditing and Testing (Pty) Ltd.) using an Agilent 6890 GC-FID. An Agilent J&W GC column CP-SIL 88 was used for the separation of the FAME components. Due to the unavailability of the instrument at CSIR the FAME analysis for sample BD02 was performed at the Tshwane University of Technology using a Varian Crompack CP-3800 gas chromatograph. A Restek Rtx-2330 column was used for the separation of the FAME components.

Quantification was performed by internal standard calibration using methyl heptadecanoate. Identification of the FAMEs in the biodiesel samples was accomplished by comparing their retention times to a Supelco FAME reference mixture containing 37 components. The FAME content was computed according to EN 14103 [16] and Ruppel and Huybrighs [17]. All the peaks from that for methyl myristate (C_{14}) to that for the methyl ester of nervonic acid ($C_{24:1}$) were accounted for. Additional biodiesel physical properties were determined, using standard procedures, by Bio Services CC, Randburg, South Africa. These properties included free glycerine, methanol content, water content, acid value, iodine value, and flash point.

2.4. Antioxidant formulations and determination of the oxidative induction times

The effect of antioxidant combinations on the induction time was determined by spiking the biodiesel with different amounts of the antioxidants keeping the total antioxidant dosage constant at 0.15 wt.%. In particular, Orox PK, Naugard P and Anox 20 binary mixtures, as well as a ternary blend, were tested. The oxidation stability of the biodiesel samples was determined on a Metrohm 895 Professional PVC Thermomat according to the Rancimat method described in EN14112 [13]. The oxidation tests were done at a constant temperature of 110°C and an airflow rate of 10 L h^{-1}. Biodiesel samples (3.00 g) were weighed into the reaction vessels, and placed in the heated cellblock. The air was passed through the sample and then through a measuring vessel that containing 60 mL of deionized water. The volatile acids formed during the oxidation process were trapped in this water causing an increase its conductivity. The change in the conductivity was continuously recorded as a function of time. Duplicate runs, and in some cases triplicate runs were conducted on each sample tested.

2.5 Data reduction

The Rancimat instrument produces data corresponding to the initial part of the oxidation reaction. The induction time values were extracted from the experimental conductivity *vs*. time data using the method described previously [15]. The conductivity *vs*. time curves ($\sigma = \sigma(t)$) were fitted using the following equation:

$$\sigma(t) = \sigma_{min} + mt + \beta F(t) \quad (1)$$

where $\sigma(t)$ is the experimental conductivity *vs*. time curve; σ_{min} is the conductivity offset at time $t = 0$; m is the slope of the initial portion of the conductivity curve; β is a proportionality constant with conductivity units and $F(t)$ is an appropriate response function that is dimensionless. The parameter m in equation (1) compensates for any linear signal drift over

the full measurement time. The response function $F(t)$ should be able to adequately represent the experimental data over the full measurement range. The following empirical expression was found adequate for the present data set [15]:

$$F(t) = log\left[1 + (t/\tau)^{\theta}\right] \quad (2)$$

where t is the time in h, "*log*" represents the natural logarithm while θ and τ are adjustable model parameters. The parameter θ is a dimensionless shape factor while τ is a characteristic time constant for the response function and therefore has units of time. These adjustable parameters of the analytic expression for $F(t)$, as well as the values of both m and σ_{min} were determined by least square fits of equation (1) to the experimental conductivity *vs*. time data.

Induction times can be estimated according to two different procedures [15]. The "manual method" (IP_T) described in EN14112 [13] corresponds to the intersection of the tangent line, drawn to the inflection point of the normalized response curve, with the time axis [18]. This leads to the following expression for the induction time in terms of the model parameters:

$$IP_T = \tau f_T(\theta) = \tau(\theta - 1)^{1/\theta}[1 - log(\theta)/(\theta - 1)] \quad (3)$$

The "automatic instrument" procedure (IP_D) mentioned in EN14112 [13] is established by finding the position of the maximum in the second derivative of the fitted $F(t)$ curve, i.e. $F''(t)$. The induction time corresponding to this second methodology is given by:

$$IP_D = \tau f_D(\theta) = \tau\left[(1/4)\left(\theta^2 + \left(3 - \sqrt{\theta^2 + 6\theta - 7}\right)\theta - 4\right)\right]^{1/\theta} \quad (4)$$

3. Results

3.1. Biodiesel characterization

The properties of the biodiesel samples used in this study are summarized in Table 1. Sample BD01 met most requirements of the EN 14214 specifications including the fact that the ester content should exceed 96.5%. This was not the case for biodiesel sample BD02. The latter was only used to study the additional combinations of the amine (Orox PK) with other phenol-type antioxidants. Note that the ester contents for samples BD01 and BD02 were determined using different GC-FID columns and instruments.

Table 1: List of biodiesel (FAME) properties made from sunflower oil.

Property	**Units**	**BD01**	**BD02**
FAME (ester content)	wt.%	98.3	94.8
FAME composition: (%)	wt.%		
Methyl palmitate, C16:0		6.73	5.82
Methyl stearate, C18:0		6.63	7.17
Methyl oleate, C18:1		22.4	16.5
Methyl linoleate, C18:2		62.0	68.2
Methyl linolenate, C18:3		0.22	0.63
Other methyl esters		2.02	1.55
Density at 15°C	kg m^{-3}	888	888
Kinematic viscosity at 40°C	mm^2s^{-1}	4.6	4.59
Flash point	°C	170	n.d.
Water content	%	0.04	0.04
Acid value	mg KOH g^{-1}	0.1	0.06
Methanol content	wt.%	0	0
Iodine value	-	118	125
Free glycerol	wt.%	0.01	0.02
Appearance	-	clear	clear

3.2. Rancimat oxidative induction periods

The effect of antioxidant combinations, on the induction time, was determined at a fixed total antioxidant concentration constant of 0.15 wt.%. The composition of the antioxidant mixture was represented in vector form (x_1;x_2;x_3) with the x_i representing the mass fractions of the individual additives present in the antioxidants package. Figure 1 shows representative conductivity vs. time data obtained with the Rancimat method. The symbols show experimental data obtained in duplicate runs and the lines correspond to least square fits of equation (1). The induction times IP_T and IP_D were calculated using equation (3) and equation (4) respectively. Table 2 lists the measured Rancimat induction IP_T and IP_D times. In most instances: $IP_D > IP_T$. The mean and standard deviation of the ratio of these values for the samples spiked with antioxidant was $IP_T / IP_D = 1.04 \pm 0.07$. The rest of the discussion focuses on IP_T values as these tended to give conservative results. Figure 2 shows the variation of the IP_T induction times, extracted from such curves, with composition for the antioxidant mixtures.

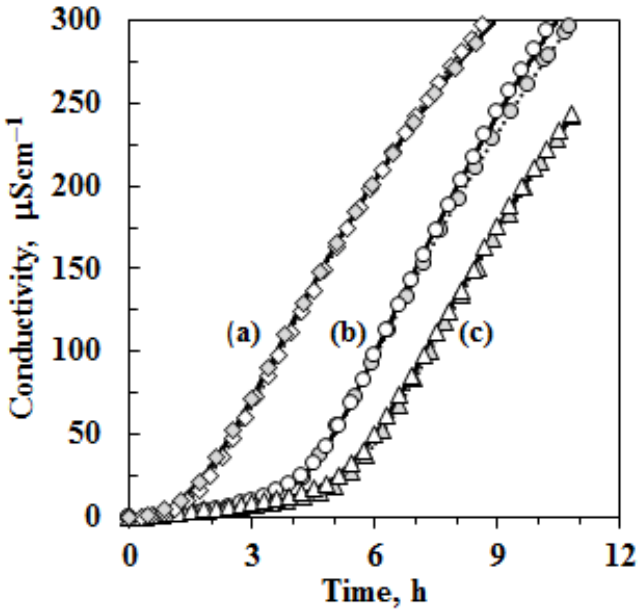

Figure 1. Representative baseline corrected Rancimat conductivity vs. time curves. The symbols represent experimental data and the solid lines are fits to the log-logistic equation. (a) Neat biodiesel; (b) 0.15 wt.% Anox 20; (c) 0.05 wt.% Orox PK with 0.10 wt.% Anox 20. The symbols indicate experimental results determined in duplicate and the solid and broken lines model fits.

Table 2. Average Rancimat Induction times (*IP*) of biodiesel spiked samples

Antioxidant weight fractions			Induction times (h)	
Orox PK	**Naugard P**	**Anox 20**	IP_T	IP_D
1.000	0.000	0.000	2.37	2.20
			2.52	2.36
0.667	0.333	0.000	1.98	1.79
			2.21	2.21
0.500	0.500	0.000	1.95	1.80
			1.88	1.81
0.333	0.667	0.000	1.85	1.79
			1.77	1.66
0.000	1.000	0.000	1.84	1.69
			1.88	1.73
0.000	0.667	0.333	2.94	3.01
			2.91	2.99
0.000	0.500	0.500	3.54	3.64
			3.48	3.56
0.000	0.333	0.667	3.79	3.88
			4.02	4.12
0.000	0.000	1.000	4.17	4.28
			4.32	4.43
0.333	0.000	0.667	5.38	5.51
			5.28	5.40
0.500	0.000	0.500	4.72	4.82
			4.82	4.92
0.667	0.000	0.333	4.22	4.33
			4.11	4.21
0.333	0.333	0.333	3.69	3.77
			3.88	3.98
Neat biodiesel			1.55 ± 0.21	1.33 ± 0.28

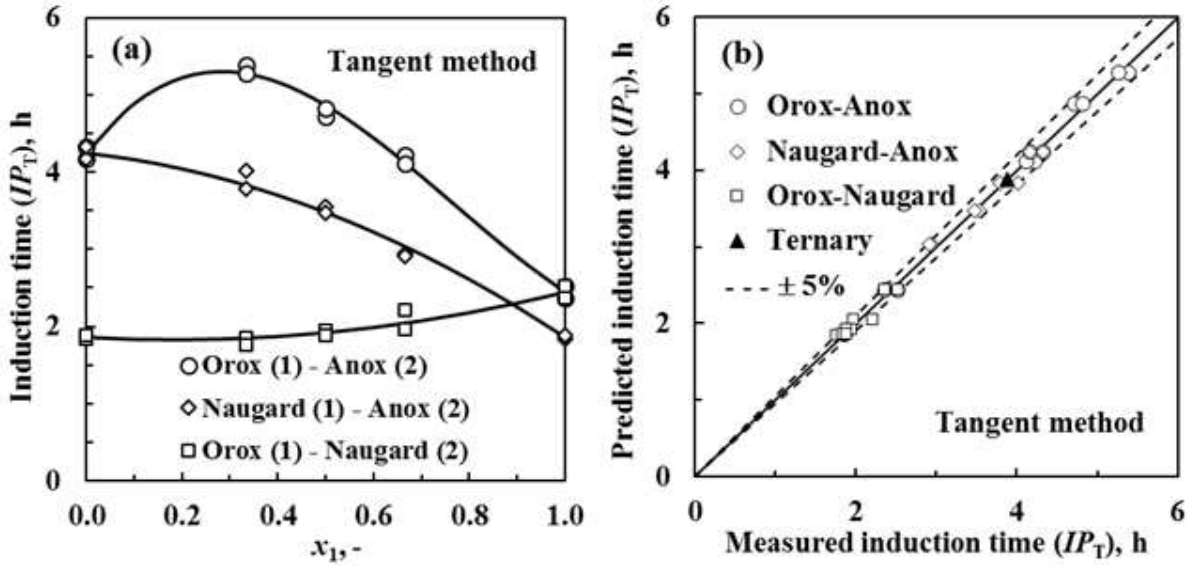

Figure 2. Measured and predicted Rancimat induction times based on the tangent method for blends of Naugard P, Anox 20 and Orox PK. The total antioxidant content was fixed at 0.15 wt.%. The variable x_1 indicates the mass fraction of first mentioned antioxidant in the binary antioxidant blend.

The composition dependence of the experimental Rancimat induction time data was fitted using Scheffé K-polynomials. Details of the fitting procedure are presented in the Appendix. The data fits in Figure 2 are indicated by the solid lines while the symbols represent actual experimental measurements. The composition dependence of the Naugard PK - Anox 20 and the Orox PK - Naugard P binaries was adequately represented by quadratic Scheffé polynomials. However, the composition dependence of IP_T for the Orox PK - Anox 20 binary was highly nonlinear, so much so that a cubic Scheffé polynomial had to be employed to fit the data. According to Table 2 and Figure 2, the hindered phenol, Anox 20, was the most effective stabilizer for the present sunflower biodiesel followed by Orox PK. None of the neat antioxidants achieved the 8 h EN14214 [19] stability requirement. However, Anox 20 on its own did exceed the 3 h ASTM D6751 [20] specification. Mixtures of Orox P and Anox 20 showed strong synergism. Virtually all combinations of these two antioxidants tested, featured IP_T values than were higher than those measured for Anox 20 on its own. The fitted curve, defined by a cubic Scheffé polynomial, predicted a maximum value of IP_T = 5.30 h at approximately a 1:2 ratio of Orox to Anox.

According to Becker and Knorr [21] synergism in a binary antioxidant combination is evident when the mixture proves to be more effective than expected, i.e. if it exceeds the sum of the induction periods recorded for the individual antioxidants acting on their own at the mixture dosage level minus the induction period of the pure biodiesel. However, these authors only observed added effects for combinations of monophenols or bisphenols with either sulfides or aromatic phosphites. Gatto and Grina [10] previously observed synergy (at approximately the same ratio found presently) of an amine antioxidant to a phenolic one in a sulfur-free mineral oil. The mechanisms responsible for this synergistic antioxidant interaction are expected to be complex and their elucidation is beyond the scope of the present investigation. However, it is likely that it can be attributed to some type of regeneration of the more effective antioxidant

by the other one, or the sacrificial oxidation of the latter to protect the former [5, 10, 12]. According to Becker *et al.* [22], while the action of chain breaking, free radical scavenging, antioxidants are fairly well understood, the mechanisms proposed to explain antioxidant synergism or antagonism are speculative and conflicting observations have been reported [23-25].

3.3 Antioxidant synergy between Orox PK and other phenolic-based compounds

Synergy was exhibited by the combination of the amine-based antioxidant Orox PK with the phenolic antioxidant Anox 20 because some mixture combinations provided more effective oxidation stabilization than the two parent compounds. It was therefore of interest to explore whether this synergy extends to mixtures of the amine with other phenolic antioxidants. Towards this end, the sunflower biodiesel was spiked with mixtures of Orox PK with several other phenolic antioxidants, at a mass ratio of 1:2. The total antioxidant concentration was kept constant at 0.15 wt.%. The phenolic antioxidants considered were TBHQ, DTBHQ, BHT, pyrogallol (PY) and propyl gallate (PG). The results for the neat and combined antioxidants are presented in Figure 3. It reveals that induction times greater than 8 h, in accordance with the EN 14214 [19] requirement, were achieved using the neat antioxidants TBHQ, PY and PG. However, only the Orox PK - DTBHQ combination possibly showed an improvement in the IP value indicative of synergism. However, the difference is not statistically significant as the error bars shown in Figure 3 overlap. Nevertheless, none of the other combinations showed any synergistic effect.

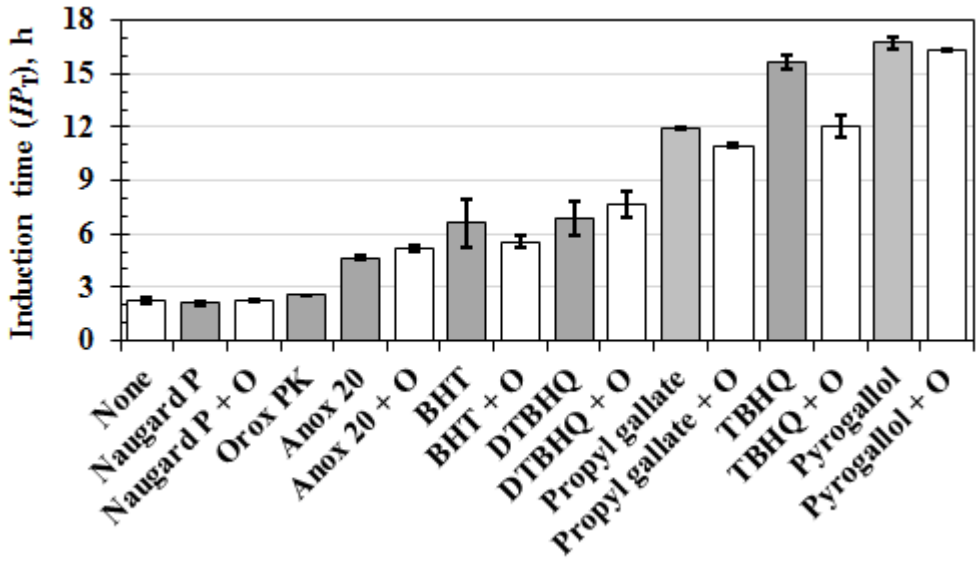

Figure 3. IP_T values for neat antioxidants and combinations with Orox PK

The induction time IP_T generally gave lower values than IP_D, especially for the more highly stabilized biodiesel samples. This means that, compared to IP_D, the IP_T values provided conservative estimates for the oxidative stabilization. This index was therefore selected for further study as it returned conservative values for biodiesel samples stabilized with antioxidants. The expressions for the estimation of induction periods, from the parameters of the response curve $F(t)$ of Equation (1), both take the form $IP_i = \tau f_i(\theta)$. This means that the ratio of the two IP values is independent of the time constant τ and given by:

$$\frac{IP_D}{IP_T} = \frac{\left[(1/4)\left(\theta^2 + \left(3-\sqrt{\theta^2+6\theta-7}\right)\theta-4\right)\right]^{1/\theta}}{(\theta-1)^{1/\theta}[1-log(\theta)/(\theta-1)]} \quad (5)$$

Figure 4 shows a plot of the IP_D/IP_T ratio. According to equation (5), IP_T exceeds IP_D when θ < 3.88. The two estimates agree to within 5 % provided θ > 3.17 and the difference is less than 2 % for θ > 4.8.

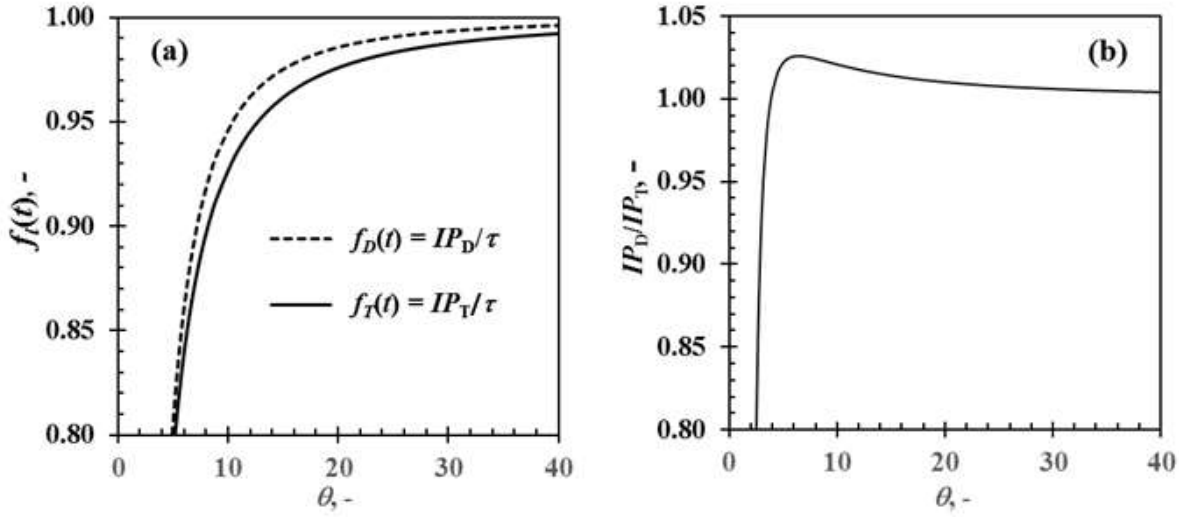

Figure 4. Plots of (a) $f_i(\theta) = IP_i/\tau$ and (b) the variation of IP_D/IP_T with the shape parameter θ.

5. Conclusion

Sunflower biodiesel was stabilized with three different antioxidants representing three different chemistries at a fixed dosage level of 0.15 wt.%. The oxidative stability was quantified using the Rancimat induction period estimated from the response curve using both the tangent method (IP_T) and the second derivative method (IP_D). It was found that, for well-stabilized biodiesel samples, $IP_D > IP_T$. The implication is that the tangent method yields conservative estimates for the induction period of stabilized sunflower biodiesel.

Synergy, with respect to stabilizing sunflower biodiesel against oxidative degradation, was detected in binary mixtures of Orox PK with Anox 20. However, mixture of Orox PK with other, more effective, phenolic-type antioxidants, in a 1:2 mass ratio, did not show such an effect. However, the best stabilization performance was obtained with pyrogallol, TBHQ and propyl gallate. On their own and in combination with Orox PK, they all yielded stabilization performance exceeding the requirement of $IP > 8$ h set by European Standard EN 14112.

Acknowledgements

Financial support for this research, from the Energy Institutional Research Theme of the University of Pretoria, is gratefully acknowledged.

Conflicts of interest

The authors declare that there are no conflicts of interest to disclose.

References

[1] G. Karavalakis, S. Stournas, D. Karonis, Evaluation of the oxidation stability of diesel/biodiesel blends, Fuel, 89 (2010) 2483-2489.
[2] G. Knothe, Some aspects of biodiesel oxidative stability, Fuel Processing Technology, 88 (2007) 669-677.
[3] S. Jain, M.P. Sharma, Stability of biodiesel and its blends: A review, Renewable and Sustainable Energy Reviews, 14 (2010) 667-678.
[4] S. Schober, M. Mittelbach, The impact of antioxidants on biodiesel oxidation stability, European Journal of Lipid Science and Technology, 106 (2004) 382-389.
[5] R. de Guzman, H. Tang, S. Salley, K.Y.S. Ng, Synergistic Effects of Antioxidants on the Oxidative Stability of Soybean Oil- and Poultry Fat-Based Biodiesel, Journal of the American Oil Chemists' Society, 86 (2009) 459-467.
[6] J. Pullen, K. Saeed, An overview of biodiesel oxidation stability, Renewable and Sustainable Energy Reviews, 16 (2012) 5924-5950.
[7] I.M. Rizwanul Fattah, H.H. Masjuki, M.A. Kalam, M.A. Hazrat, B.M. Masum, S. Imtenan, A.M. Ashraful, Effect of antioxidants on oxidation stability of biodiesel derived from vegetable and animal based feedstocks, Renewable and Sustainable Energy Reviews, 30 (2014) 356-370.
[8] M. Chao, W. Li, X. Wang, Antioxidant synergism between synthesised alkylated diphenylamine and dilauryl thiodipropionate in polyolefin base fluid, Journal of Thermal Analysis and Calorimetry, 117 (2014) 925-933.
[9] E. Marinova, A. Toneva, N. Yanishlieva, Synergistic antioxidant effect of α-tocopherol and myricetin on the autoxidation of triacylglycerols of sunflower oil, Food Chemistry, 106 (2008) 628-633.
[10] V. Gatto, M. Grina, Effects of base oil type, oxidation test conditions and phenolic antioxidant structure on the detection and magnitude of hindered Phenol/Diphenylamine synergism, Lubrication Engineering, 55 (1999) 11-20.
[11] K.U. Ingold, Inhibition of the autoxidation of organic substances in the liquid phase, Chemical Reviews, 61 (1961) 563-589.
[12] E.A. Decker, Antioxidant mechanisms, in: C.C.M. Akoh, D. B. (Ed.) Food lipids, Marcel Dekker Inc., New York, 2002, pp. 517-542.
[13] BS EN 14112, Fat and oil derivatives-Fatty Acid Methyl Esters (FAME)-Determination of oxidation stability (accelerated oxidation test), in, 2003.

[14] W.W. Focke, I.V.D. Westhuizen, A.B.L. Grobler, K.T. Nshoane, J.K. Reddy, A.S. Luyt, The effect of synthetic antioxidants on the oxidative stability of biodiesel, Fuel, 94 (2012) 227-233.
[15] W.W. Focke, I.V.D. Westhuizen, X. Oosthuysen, Biodiesel oxidative stability from Rancimat data, Thermochimica Acta, 633 (2016) 116-121.
[16] BS EN 14103, Fat and oil derivatives-Fatty Acid Methyl Esters (FAME)-Determination of ester and linolenic acid methyl ester contents, in, 2011.
[17] T. Ruppel, T. Huybrighs, Fatty Acid Methyl Esters in B100 Biodiesel by Gas Chromatography (Modified EN 14103).
[18] P.K. Fearon, S.W. Bigger, N.C. Billingham, DSC combined with chemiluminescence for studying polymer oxidation, Journal of Thermal Analysis and Calorimetry, 76 (2004) 75-83.
[19] European standard EN 14214, Automotive fuels-Fatty Acid Methyl Ester (FAME) for diesel engines-Requirements and test methods, in, 2012.
[20] ASTM D6751-11b, Standard specification for Biodiesel Fuel Blend Stock (B100) for Middle Distillate Fuels[1], in, 2011.
[21] R. Becker, A. Knorr, An evaluation of antioxidants for vegetable oils at elevated temperatures, Lubrication Science, 8 (1996) 95-117.
[22] E.M. Becker, G. Ntouma, L.H. Skibsted, Synergism and antagonism between quercetin and other chain-breaking antioxidants in lipid systems of increasing structural organisation, Food Chemistry, 103 (2007) 1288-1296.
[23] R.K. Jensen, S. Korcek, M. Zinbo, J.L. Gerlock, Regeneration of amine in catalytic inhibition of oxidation, The Journal of Organic Chemistry, 60 (1995) 5396-5400.
[24] E.T. Denisov, Cyclic mechanisms of chain termination in the oxidation of organic compounds, Russian Chemical Reviews, 65 (1996) 505-520.
[25] E.A. Haidasz, R. Shah, D.A. Pratt, The catalytic mechanism of diarylamine radical-trapping antioxidants, Journal of the American Chemical Society, 136 (2014) 16643-16650.

Appendix. Correlating ternary mixture data with Scheffé K-polynomials

Consider a mixture that contains q different components. Let the x_i be fractions that describe the mixture composition. In the present example this is achieved by choosing mass fractions as the composition variables. The question is to develop consistent expressions that connect mixture composition with a mixture property. In the present case, the "property" is the effect the mixture has on the oxidative stability of a biodiesel when it is added at a fixed dosage of 0.15 wt.%.

The Scheffé K-polynomials are the most common empirical models applied in the context of experimental mixture design. In essence they are trimmed Taylor polynomials that take the mixture constraints into account, i.e.:

$0 \le x_i \le 1$ for $i = 1, 2, \ldots. q$ (A-1)

Together with the simplex constraint

$$\sum_1^q x_i = x_1 + x_2 + \cdots + x_q = 1 \quad \text{(A-2)}$$

The n^{th}-order Scheffé K-polynomials are homogeneous first order in the model parameters and homogeneous n^{th}-order in the composition variables. The mixture property is denoted by a_{mix} and the model parameters by a_i, a_{ij}, and a_{ijk} depending on the order of the K-polynomial. Note that irrespective of order of the model that is used, the property value for pure component i is given by $a_i = a_{ii} = a_{iii} \ldots$ The present study considered a ternary mixture of antioxidants so $q = 3$ and the mixture property of interest was the effect on the stability of the biodiesel as quantified by the Rancimat induction time IP_T.

The first order Scheffé polynomial for a ternary mixture is given by:

$$a_{mix} = a_1 x_1 + a_2 x_2 + a_3 x_3 \quad \text{(A-3)}$$

This is the so-called "linear blending rule" and it states that the mixture property varies linearly with composition. In effect the mixture property is defined by a composition weighted arithmetic mean over the pure component properties. The key advantage of the linear blending rule is that pure component properties suffice to predict multicomponent behavior.

The second order Scheffé K-polynomial for a binary *i-j* mixture is described by:

$$a_{mix} = a_{ii}x_i^2 + 2a_{ij}x_i x_j + a_{jj}x_j^2 \qquad \text{(A-4)}$$

In this model the parameter a_{ij} describes interaction effects. A q-component mixture will comprise $q(q\text{-}1)$ different binaries and thus the model will feature that number of binary interaction parameters. In addition, binary experimental data is required to fix these parameters. Once known, multicomponent property values can be predicted.

The experimental IP values obtained for the Orox-Naugard and Naugard-Anox binary blends were such that the composition dependence was adequately represented by second order Scheffé polynomials. However, the response for the Orox-Anox binary was highly nonlinear and it was necessary to use a cubic Scheffé K-polynomial to correlate the data for this system. This means that the ternary data for the system Orox (1) - Naugard (2) - Anox (3) system must also be fitted with a third order Scheffé polynomial:

$$a_{mix} = a_{111}x_1^3 + 3a_{112}x_1^2x_2 + 3a_{113}x_1^2x_3 + a_{222}x_2^3 + 3a_{122}x_1x_2^2 + 3a_{223}x_2^2x_3 + a_{333}x_3^3 + 3a_{133}x_1x_3^2 + 3a_{233}x_2x_3^2 + 6a_{123}x_1x_2x_3 \qquad \text{(A-5)}$$

Where $a_{mix} = IP_T$ is the induction time in the presence of the antioxidant blend at a fixed dosage of 0.15 wt.%; x_i represents the mass fraction of additive *i* in the antioxidant blend; a_{iii} is the Rancimat induction time recorded for neat antioxidant *i*, and the a_{ijk} are adjustable model parameters. Note that a cubic Scheffé polynomial features two binary interaction parameters for each binary and one ternary parameter for each ternary in the system. So, for the present case there are six binary parameters a_{ijj} (or a_{iij}) and one ternary constant a_{123} to be

determined. Thus it would appear that there are a total of ten parameters that need to be fixed. However, as already mentioned, the data for two of the binaries were adequately fitted by the lower order quadratic Scheffé model. Now, a convenient aspect of Scheffé polynomials is the fact that they form a set of nested models that range from the linear bending rule to whatever order is desired. Lower order models can be transformed into higher order ones by multiplication with the simplex constraint, equation (A-2). This allows the "upgrading" of lower order models for incorporation into one of a higher order model without increasing the number of parameters to be fixed. In the present case the upgrading of the quadratic, described by equation (A-4), to the cubic form is achieved by multiplying the right hand sided with $x_i + x_j = 1$:

$$a_{mix} = a_{ii}x_i^3 + (a_{ii}+2a_{ij})x_i^2x_j + (a_{jj} + 2a_{ij})x_ix_j^2 + a_{jj}x_j^3 \qquad \text{(A-6)}$$

Comparing coefficients shows that $a_{iii} = a_{ii}$; $3a_{iij} = a_{ii} + 2a_{ij}$, etc. So the ternary parameters are expressed in terms of specific combinations of the binary and pure component parameters. This means that, for the present case, only eight model parameters were required to fit the cubic Scheffé polynomial to the mixture data. Taking this into account, the following procedure was used to fix the model parameters. The neat component parameters a_{iii} were determined as the average of the two measurements for the effect of the neat antioxidants. The rest of the parameters were determined by least square data fitting. Table 3 lists the final parameter values. The solid lines drawn in Figure 2(b) in the main text show the IP values predicted with the full ternary model. Note that similar data fits were used to correlate the response function parameters, θ and τ, to antioxidant mixture composition. The results are also shown in Table 3.

Table 3. Orox (1) – Naugard (2) – Anox (3) antioxidant package Scheffé cubic model for the prediction of IP_T and for correlating the composition dependence of the parameters of the response function.

IP_T composition dependence									
a_{111}	a_{222}	a_{333}	a_{112}	a_{113}	a_{122}	a_{133}	a_{223}	a_{233}	a_{123}
2.446	1.860	4.247	1.940	3.805	1.745	6.932	3.223	4.018	5.180
Equation (2) model parameter composition dependence									
τ_{111}	τ_{222}	τ_{333}	τ_{112}	τ_{113}	τ_{122}	τ_{133}	τ_{223}	τ_{233}	τ_{123}
4.233	3.322	4.861	3.136	3.276	2.832	7.817	3.896	4.409	4.584
θ_{111}	θ_{222}	θ_{333}	θ_{112}	θ_{113}	θ_{122}	θ_{133}	θ_{223}	θ_{233}	θ_{123}
3.053	2.959	7.061	3.340	9.533	3.308	9.480	5.618	6.985	4.665